



Titanium dioxide based strategies to prevent algal fouling on cementitious materials

Anibal Maury-Ramirez^a, Willem De Muynck^{a,b}, Ruben Stevens^a, Kristof Demeestere^c, Nele De Belie^{a,*}

^a Magnel Laboratory for Concrete Research, Department of Structural Engineering, Faculty of Engineering and Architecture, Ghent University, Technologiepark Zwijnaarde 904, B-9052 Ghent, Belgium

^b Laboratory of Microbial Ecology and Technology (LabMET), Department of Biochemical and Microbial Technology, Faculty of Bioscience Engineering, Ghent University, Coupure Links 653, B-9000 Ghent, Belgium

^c Research Group EnVOC, Department of Sustainable Organic Chemistry and Technology, Faculty of Bioscience Engineering, Ghent University, Coupure Links 653, B-9000 Ghent, Belgium

ARTICLE INFO

Article history:

Received 2 February 2012

Received in revised form 31 July 2012

Accepted 24 August 2012

Available online 23 September 2012

Keywords:

Autoclaved aerated concrete

Cement paste

Water repellent

Microbial growth

Algae

Self-cleaning

ABSTRACT

Algal growth is an important phenomenon largely affecting the aesthetical properties of building facades worldwide. Based on the photocatalytic degrading action together with the photo-induced hydrophilic nature of TiO₂, three TiO₂ containing white cements and one novel TiO₂ coating applied on autoclaved aerated concrete have been evaluated as strategies to avoid algal fouling on new and existing buildings, respectively. During 16 weeks (4 months), the evaluation was conducted using an accelerated algal growth test set-up running with *Chlorella vulgaris* as the algae specie. Monitoring of the fouling was based on visual inspections, algal coverage (%) and human perception of the color changes (ΔE) produced on the samples. A commercially available TiO₂ containing cement evidenced 'not visible' algal growth ($\Delta E \leq 0.2$) and almost no significant algal coverage (0.1%). The new TiO₂ based coating evidenced 20% less algal coverage compared to uncoated reference samples after the test. However, 'very large' color changes ($\Delta E = 20$) were observed on these samples.

© 2012 Elsevier Ltd. All rights reserved.

1. Introduction

Due to technical and economical factors, a large number of building envelopes are typically made of mortar or concrete. When exposed to specific environmental conditions, these building envelopes become ideal substrates for microbial colonization. This phenomenon changes the materials' aesthetical appearance and, in a later stage, even can compromise structures' durability by biologically induced corrosion or physical degradation [1,2]. The type of microorganisms found on these building envelopes differs from region to region, but research has identified algae as one of the initial and main microbial groups colonizing cement based building facades in Europe and America [3,4]. Among the traditional methods to prevent algal growth on cementitious materials, the use of biocides is common. However, most frequently due to leaching, these products do not promote long term protection and, therefore, need to be repeatedly applied [5,6]. Another technology commonly used to avoid the fixation and growth of microorganisms on building materials is the use of water repellents. Different from biocides, for which the objective is to eliminate the microorganism, the

function of water repellents is to prevent the ingress of water into the building materials on which they are applied. As a consequence, surfaces treated with a water repellent will remain wet for a shorter time compared to untreated ones. In principle, this will decrease the deposition of air pollutants, dust and the development of biological colonization. Although in most cases the application of water repellents has performed as expected, there are some practical cases (e.g. applied on autoclaved aerated concrete or marble) in which undesired effects as streaking have been reported [7–9]. Based on the aforementioned limitations, further development of innovative, more efficient and environmentally friendly strategies to protect cementitious materials from algal growth are needed.

Recently, the air-purifying properties of TiO₂ loaded cementitious materials have shown potential to improve air quality when applied in specific structures such as tunnels and pavements. Due to the degrading action of TiO₂ photocatalysis, these photocatalytic cement based materials have been reported to eliminate both organic air pollutants such as toluene [10–12] and inorganic air pollutants such as NO_x [13–15]. This photocatalytic degrading action together with the photo-induced hydrophilic nature of TiO₂ entails self-cleaning and antimicrobial properties to the material [16–21]. So far, most research on TiO₂ loaded building materials has focused on the air-purifying properties. Limited attention has been paid to their antimicrobial and self-cleaning properties. Despite the fact that photosynthetic microorganisms are the first colonizers, the

* Corresponding author. Tel.: +32 9 264 55 22; fax: +32 9 264 58 45.

E-mail addresses: anibal.mauryramirez@ugent.be (A. Maury-Ramirez), willem.demuynck@ugent.be (W. De Muynck), kristof.demeestere@ugent.be (K. Demeestere), nele.debelie@ugent.be (N. De Belie).

algicidal effect of TiO_2 loaded cementitious materials has been investigated only in very few cases. For example, a coating based on a TiO_2 dispersion, showed a photocatalytic inhibition of around 66% of the algal growth (*Oedogonium*) when applied on a cement substrate under a combination of fluorescent and black light irradiation. Higher inhibition efficiencies were found when adding 1% of noble metals such as Pt and Ir [19]. Applying a TiO_2 coating which is based on a vacuum saturation process on autoclaved aerated concrete, a reduction of approximately 40% in the algal growth was obtained after 4 weeks of testing in an accelerated algal growth test set-up under fluorescent light [18]. Similarly, to evaluate the TiO_2 effect on a mixed culture of two green microalgae (*Stichococcus bacillaris*, *Chlorella ellipsoidea*) and one cyanobacteria (*Gleocapsa dermochroa*), nanocrystalline anatase powder was applied by direct addition during the manufacturing process of different mortars, at a proportion, by volume: 12:4:4:1 – sand:lime:anatase:Portland cement. Results indicated that the antimicrobial activity from these TiO_2 added mortars was effective after 4 months of exposure to outdoor conditions. Application of the same photocatalyst within coatings onto 2 wall surfaces of the Palacio Nacional da Pena (Portugal) showed promising results concerning the degradation of lichens and other phototrophic microorganisms after two weeks of color monitoring. However, long lasting effect of this application has still to be confirmed [17]. In a longer time frame, roofing tiles (red engobe, natural clay, black varnish) coated by a sol–gel technology were evaluated while being exposed during more than 6 years to outdoor conditions in 6 different locations in Germany. Results indicated that photocatalytic surfaces did not affect phototrophic biofilms [21].

While the algicidal activity of TiO_2 loaded cementitious materials has not been explored in detail, the algicidal activity of pure TiO_2 has already been reported in scientific literature for water treatments purposes [22–24]. As a result, a preliminary degradation mechanism of the algae has been stated. The degradation mechanism begins with the photocatalytic action of the TiO_2 generated oxidative species on the protective cell structures: the cell wall, the cell membrane and organelle membranes. These must be disturbed before the *Chlorophyll* and other pigments are oxidatively transformed by the action of the TiO_2 photocatalyst. The protective wall and membranes of the cell undergo radical-induced changes. Alterations in color, in the form of *Chlorophyll* degradation do not take place readily, since the catalyst must first affect the cell's protective structures. The delay in visible color change corresponds to a mechanistic pathway that involves changes in the cell wall, cell membrane and other membrane structures prior to oxidation of pigments. This preliminary explanation of the mechanistic pathway is in agreement with TiO_2 studies reported by Peller et al. [23], Linkous et al. [19], Hong et al. [24] using algae species such as *Cladophora*, *Chroococcus*, *Oedogonium*, respectively.

As data concerning TiO_2 based strategies to avoid algal growth on cementitious materials are scarce and results in most cases have evidenced limited or no reduction of the algal growth, more research should be conducted to develop more efficient TiO_2 strategies against this phenomenon. In order to prevent algal fouling on existing structures, we proposed the use of a completely new TiO_2 coating which combines water repellency and TiO_2 photocatalytic properties. As another strategy to prevent fouling on new structures, cements containing TiO_2 in three different concentrations have been evaluated. Among these cements, at the best of our knowledge, the evaluation of selected commercially available cement added with TiO_2 has been conducted for the first time in relation to microbial growth. The antifouling behavior has been evaluated by means of an accelerated algal growth test set-up with UV-A irradiation and using *Chlorella vulgaris* as algae specie. During 16 weeks (4 months), monitoring of these TiO_2 based strategies was conducted by visual inspections, determination of the algal

coverage (%) and human perception of the color changes (ΔE) produced on the samples.

2. Materials and methods

2.1. TiO_2 loaded cementitious materials

In order to avoid algal fouling on cementitious materials, two completely different TiO_2 strategies were considered in this research. First, cements added with TiO_2 at three different concentrations were evaluated as strategy for new buildings. A cement paste (TiO_2 -C) was manufactured with a commercially available TiO_2 added white cement (CBR, Belgium). Additionally two different cement pastes containing TiO_2 (Kemira Chemicals, Finland) in concentrations of 5% (5% TiO_2) and 10% (10% TiO_2) were manufactured with a traditional architectural white cement CEM II/A-LL 42.5N (CBR, Belgium). As a reference, cement paste samples without TiO_2 (REF-P) were prepared with the same architectural white cement. In order to obtain comparable results, all cement pastes were designed to have the same water to binder ratio fixed at 0.5 (weight basis). Cement pastes samples were cast in cubic molds of 150 mm \times 150 mm \times 150 mm. After de-molding them, all cubic samples were allowed to cure at controlled temperature ($20 \pm 2^\circ\text{C}$) and relative humidity ($95 \pm 5\%$) in a curing room during 28 days. For all cement pastes, 10 mm thick slices from the outer surface of the cubic samples were cut with a surface area of 60 mm \times 150 mm.

Second, as strategy for avoiding algal fouling on existing buildings and considering our previously reported anti-fouling properties using a TiO_2 coating produced by a vacuum saturation technique (SVS) [18], a novel combination of this coating (SVS) and a water repellent (WR) was evaluated on autoclaved aerated concrete (WR-SVS). The water repellent which has silane as main active ingredient (Rubson – Henkel, Germany) was applied by brush in three layers (drying time between layers = 0.5 h). Previously, the TiO_2 suspension was applied on the samples by means of the vacuum saturation based coating technique (SVS) during 2.5 h in a vacuum tank at 100 mbar. The in-house developed TiO_2 -ethanol suspension has a concentration of 0.05 g mL^{-1} (Kemira Chemicals, Finland). More details about this coating can be found in Maury and De Belie [18]. As a comparison, the TiO_2 coating based on the vacuum saturation (SVS) and the application of water repellent alone (WR) were also evaluated during the experiments. Similarly, non-coated autoclaved aerated concrete samples were also tested as references (REF-C). Selection of the autoclaved aerated concrete as substrate for the evaluation of the novel coating WR-SVS was based on the high bioreceptivity of this material which allows a fast and clear evaluation of the algicidal activity. Samples were cut from autoclaved aerated concrete pre-cast panels (Xella, Belgium) with the following dimensions (width \times length \times height): 80 mm \times 160 mm \times 10 mm.

In this research, specimens were prepared in quadruplicates for each treatment. From these, three specimens were used for the accelerated algal growth test and one for water contact angle measurements. As the initial pH value of the surfaces of the materials was too high (above 10) to allow algal growth, the samples were subjected to ageing by accelerated carbonation prior to the start of the accelerated algal growth. This was achieved by exposing the specimens to CO_2 levels of about 10% (at $70 \pm 10\%$ relative humidity and 20°C) in a conditioning chamber (Minibox Christ. Crucke, Belgium). On a weekly basis, the pH at the surface of the samples was verified by placing a drop of demineralized water on each specimen's surface as described in ASTM F 710-08 [25]. After 5 min of contact, the pH of the water drops on each specimen surface was measured by means of a pH indicator strip (pH 9–13,

Vel N.V., Belgium). After 4 weeks, once the pH of the surfaces (water drop) amounted to about nine, all specimens were removed from the accelerated carbonation chamber. In general, carbonation results in the conversion of calcium hydroxide in cementitious materials to calcium carbonate and concomitantly in a decrease of the pH. Other physical characteristics of the specimens such as open porosity and roughness were also measured by a vacuum saturation method described in ASTM C 1202-02 [26] and roughness coefficients (R_a) calculated as indicated in BS 1134:2010 [27]. The roughness coefficient for each material was calculated as an average of more than 200 R_a coefficients (analysis length = 8 mm) obtained within 3 samples, using a laser profilometer. The open porosity (Eq. (1)) was calculated from the buoyant mass of the saturated specimen (M_b), the oven ($105 \pm 5^\circ\text{C}$)-dry (M_{od}) and the saturated surface-dry (M_{ssd}) mass of the three specimens.

$$\text{Open porosity} = (M_{ssd} - M_{od}) \times (M_{ssd} - M_b)^{-1} \times 100\% \quad (1)$$

2.2. Titanium dioxide

A quantitative X-ray diffractometric analysis was conducted (GEOS, Belgium) on the commercially available TiO_2 added cement ($\text{TiO}_2\text{-C}$) in order to determine the TiO_2 crystal type and also the amount of TiO_2 present. The sample was mixed with an internal standard (zincite) and measured by X-ray diffraction ($\text{CuK}\alpha$ radiation). The quantification of the TiO_2 fraction in the cement was done then by modeling (based on Rietveld's Method). Similarly, the specific surface area and type of TiO_2 used for the TiO_2 coatings (SVS and WR-SVS) and added cement pastes (5% TiO_2 and 10% TiO_2) was confirmed by a volumetric N_2 -gas adsorption method (BET, Belsorp-mini II, Japan) and an X-ray diffractometric analysis (Siemens D5000, Germany) on the supplied TiO_2 nanopowder ANX Type N100 (Kemira Chemicals, Finland).

2.3. Algae culture

Based upon representativeness and ease of liquid culture, *Chlorella vulgaris* var. *viridis* chodat., was the algae species selected in this research. The strain was obtained from the culture collection of algae and protozoa (CCAP) from Dunstaffnage Marine Laboratory (Scotland, UK) (accession number CCA 211/12). Batch cultures of the algae were grown under sterile conditions in Erlenmeyers containing 1 L of Walne medium with addition of 0.2 mg thiamine chlorhydrate and 0.01 mg vitamin B12. The Erlenmeyers were continuously exposed to light by means of Grolux 30 W lamps (Sylvania, Germany) on a KS 501 rotary shaker (Ilka Werke, Germany) at 100 rpm. Air was provided by means of an Air plus 3 air pump (Project blue, Italy). For the preparation of the medium, 1 mL of sterile concentrated Walne and 0.1 mL of vitamin solution were added to 1 L autoclaved mineral water (Cristaline, natural spring water, Mèrignies, France). Each week, new batch cultures were grown by transferring 150 mL of the one week old culture to 1 L of fresh medium. The remaining culture solution was used to inoculate the PET bottles used in the accelerated algal growth test set-up. The amount of cells per mL was determined by means of a Zeiss Axioskop II plus light microscope (Zeiss, Germany) and a counting chamber.

2.4. Accelerated algal growth test set-up

The accelerated algal growth on the samples was achieved by means of a water run-off test developed in house by De Muynck et al. [7]. This modular test set-up (Fig. 1) was designed to allow simultaneous evaluation of different strategies to minimize algal growth on cement based materials. It consists of inclined (45°)

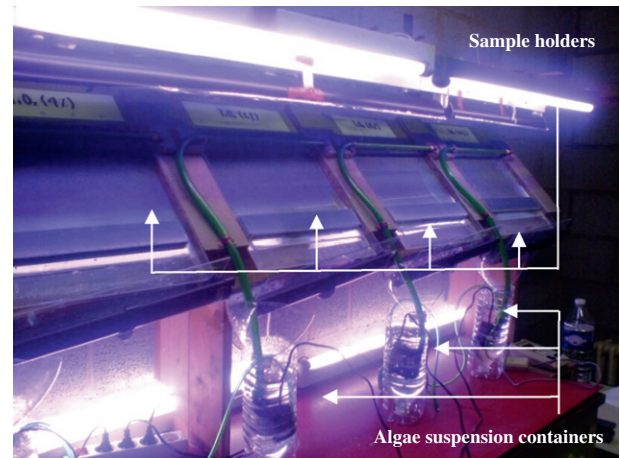


Fig. 1. Accelerated algal growth test set-up with UV-A irradiation.

and independent PVC compartments where samples are placed (sample holder) and subjected to two daily (every 12 h) alternate wet cycles (algae suspension 6.5×10^8 cells L^{-1}) lasting 1.5 h. Furthermore, as algae are photosynthetic microorganisms, their growth is also stimulated by creating a 12 h day and night regime, which started simultaneously with the run-off periods. Day regimes were created by a combination of fluorescent Grolux 30 W lamps that are specially designed to assist algal growth (Sylvania, Germany). Irradiation peaks from this lamp type are at 365, 400, 550 and 580 nm. In addition to the previously described lamps (fluorescent Grolux 30 W lamps) we added UV-A lamps type BLB TL-D 36 W (Philips, Holland) to activate the photocatalytic action. Irradiation peaks from this lamp type are at 352 and 368 nm. Measured by a UV radiometer with a sensor calibrated at 365 nm (UVP, USA), irradiation level averages on all specimens at the test set-up ranged from $0.5 \pm 0.2 \text{ mW cm}^{-2}$ at the lowest part to $1.4 \pm 0.3 \text{ mW cm}^{-2}$ at the highest part. On the other hand, as darkness triggers other cell activities, algae need several hours of darkness a day. Therefore, during the night regime, all light systems were off. Finally, for creating a suitable environment for the algal growth process, the accelerated algal growth test set-up was placed inside a room with high relative humidity (RH). By means of a thermo-hygrometer sensor (Logger Testo 175-H2), RH and temperature were continuously monitored during the whole test. Temperatures ranged between 24.2°C (day) and 20.6°C (night). Similarly, RH ranged between 82.4% (day) and 92.4% (night).

2.5. Evaluation of the algal growth on test specimens

As the problem of algal growth on cement based materials has important consequences in the aesthetical properties of building materials, human visual inspection (images) could be enough to judge the strategies to avoid algal growth (e.g. TiO_2 photocatalysis). However, in order to avoid human's eye subjectivity, two quantitative criteria which are based on the CIE Lab color space (L^* , a^* , b^* coordinates) were used besides visual inspection. On one hand, as algal growth on cement based materials can be a localized or global problem on the materials surfaces, the algal coverage on the specimens is determined by means of image analysis. On the other hand, due to *Chlorophyll* presence, algal growth quality is related with the green intensity of the colonized area. Therefore, analysis of color changes on the surface of the specimens is conducted by means of colorimetric measurements. In this research, all monitoring data during the accelerated algal growth process on the test specimens were taken on a weekly basis.

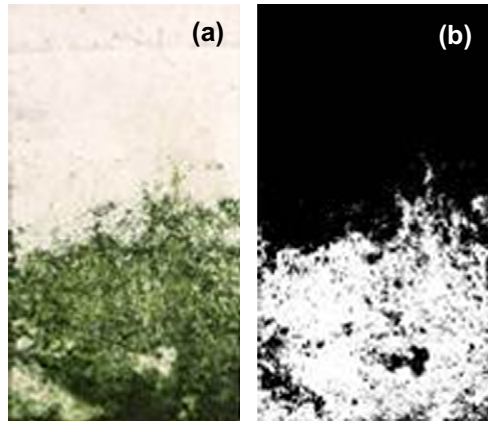


Fig. 2. Image analysis on a reference sample from the paste specimen (REF-P) before (a) and after (b) thresholding.

The algal coverage or fouled area was calculated by means of image analysis of the test specimens. Images from each specimen were obtained with the use of a scanner LiDE 70 (Canon, Vietnam). These images were subsequently processed by means of Image J 1.38x software [28]. The quantification of the algal coverage was based on a threshold analysis from the b^* coordinate (blue to yellow axis) from the CIE Lab color space. Fig. 2 shows the image analysis of one reference paste specimen as an example. Pixels with b^* values below 138 on a scale of (0–256) were considered as unfouled area (changed to black pixels), while those with b^* values above 138 were regarded as algal coverage (changed to white pixels). Similarly, this threshold value amounted 128 for autoclaved aerated concrete specimens. The total amount of black and white pixels was then calculated by means of the ‘analyze, histogram’ function for each sample. From the latter, the percentage of algal coverage can be calculated as indicated in Eq. (2). More details about this methodology can be found in De Muynck et al. [7].

$$\text{Covered area(\%)} = (\text{white pixels} \times (\text{white pixels} + \text{black pixels})^{-1}) \times 100\% \quad (2)$$

In order to evaluate the color changes on the test specimens, colorimetric measurements were performed by means of an X-Rite SP60 colorimeter with an 8 mm aperture (X-Rite, USA). On each specimen, 3 measurements were taken before and during the accelerated algal growth test. Measurements were conducted at standardized positions in the upper, middle and lower part of the specimen. Furthermore, in order to avoid the influence of the humidity of the samples in these measurements, the samples were surface-dried during 2 h at 25 °C and 60% RH before any color measurement. From these colorimetric measurements, CIE Lab color values were obtained. In order to have a complete analysis of all color changes produced by algal growth, a color change parameter (ΔE) was calculated as indicated in the following equation:

$$\Delta E = (\Delta L^2 + \Delta a^2 + \Delta b^2)^{1/2} \quad (3)$$

Being $\Delta L = L_t^* - L_0^*$; $\Delta a = a_t^* - a_0^*$; $\Delta b = b_t^* - b_0^*$ with L_t^* , a_t^* , b_t^* being color values at specific week (t) and L_0^* , a_0^* , b_0^* color values before starting the test (samples not fouled). Based on the computer simulation that estimates the human perception of the color changes (ΔE) after the aesthetic rehabilitation of architectural concrete, the produced color changes on the paste specimens could be assessed following the parameters indicated in Table 1 [29].

2.6. Water contact angle measurements

In order to evaluate the wettability of the samples prepared with the different TiO_2 strategies (coatings and additions), a

Table 1

Human perception of color changes after aesthetic rehabilitation of architectural concrete based on ΔE values [29].

Color change (ΔE)	Human perception
0.0–0.2	Not visible
0.2–0.5	Very slight
0.5–1.5	Slight
1.5–3.0	Obvious
3.0–6.0	Very obvious
6.0–12.0	Large
≥ 12	Very large

FTA2000 set-up (First Ten Angstroms, Inc., USA) was used before, during and after UV-A irradiation. For both strategies, UV-A irradiation was provided in two different ways. For the coatings, UV-A irradiation was supplied during 24 h by means of a UV-A cabinet C-75 (UVP, USA) with an UV-A irradiation intensity of $1.8 \pm 0.4 \text{ mW cm}^{-2}$. Due to the high water absorption of the samples, measurements were only performed on samples containing water repellent (WR and WR-SVS), and after 3 s of the drop release. In the case of the cement pastes, measurements were only performed after exposure of the samples to the algal growth test set-up ($0.5\text{--}1.4 \text{ mW cm}^{-2}$ UVA) during 16 weeks. As the existence of water proofing compounds in the samples prepared with the commercially available TiO_2 added white cement (TiO2-C) was not known, water contact angle measurements were performed after 1 and 10 s of the drop release. For comparative purposes, the wettability of the reference samples (REF-C) was also studied. In all cases, water contact angle measurements were calculated making averages of the angles (right and left) from three different water drops (Mili-Q quality) with a volume of 5 μL each.

2.7. Statistical analysis

Experiments were at least performed in triplicate ($n = 3$). Error bars on graphs and values in tables present the standard deviation. Comparison of mean values was done by using one-way Anova analysis. Statistical software SPSS 19.0 was used for this purpose. Grouping of treatments based on significant differences in mean values was done according Student Newman Keuls or Dunnet T3 tests ($p = 0.05$), depending on homoscedasticity results of the Levene test.

3. Results and discussion

3.1. Algal fouling on cementitious materials

Cement paste (REF-P, 5% TiO_2 , 10% TiO_2 and TiO_2 -C) and autoclaved aerated concrete samples (REF-C, SVS, WR, WR-SVS) exhibited large differences in the rate and intensity of algal fouling as can be observed in Figs. 3–5. The higher rate of fouling observed on autoclaved aerated concrete samples compared to the cement paste ones can be attributed to the high bioreceptivity of this concrete (indicated by porosity and roughness) as can be observed in Table 2.

3.2. Algal fouling on cement paste samples

The samples prepared with the commercially available TiO_2 added cement (TiO2-C) exhibited much larger algicidal activity compared to cement paste samples to which TiO_2 was added in 5% and 10% dosages (5% TiO_2 and 10% TiO_2) (Figs. 3a–5a). After 16 test weeks, algal coverage results (0.1%) on samples TiO2-C indicated a complete elimination of the algal fouling, while fouling

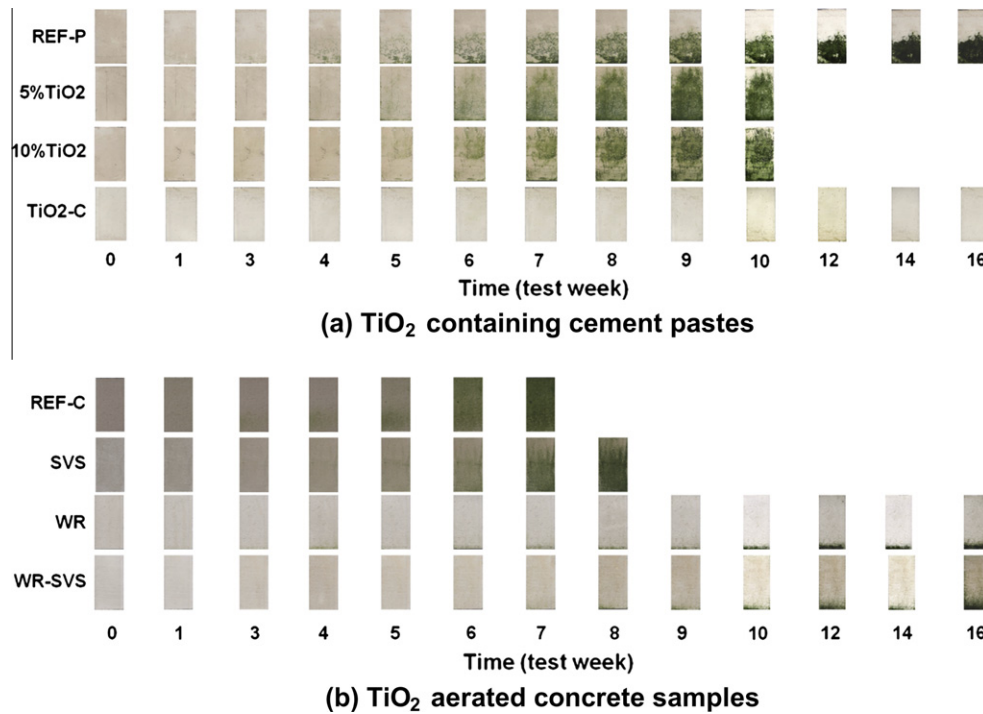


Fig. 3. Evolution of the visual appearance of (a) TiO_2 containing cement pastes and (b) TiO_2 coatings applied on autoclaved aerated concrete during the accelerated algal growth test.

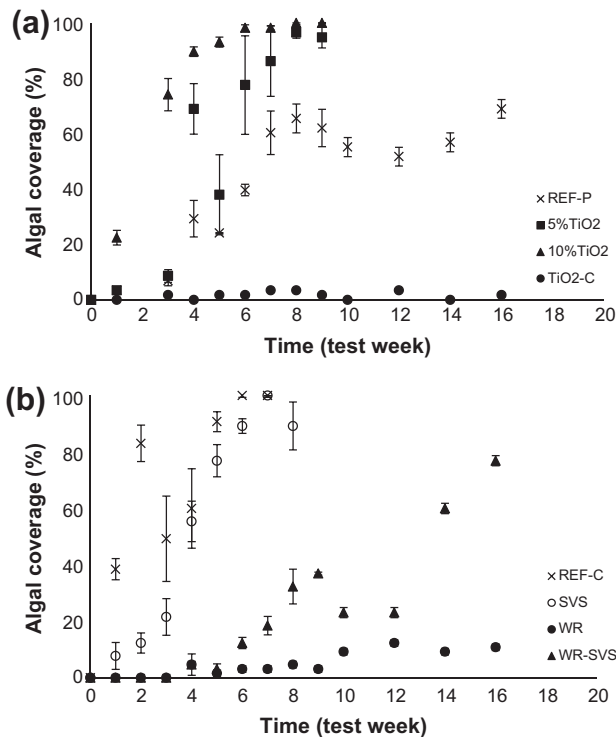


Fig. 4. Evolution of the algal coverage on different (a) TiO_2 containing cement pastes and (b) TiO_2 coated autoclaved aerated concrete samples ($n = 3$).

of the complete surface (over 80%) was observed using the laboratory manufactured TiO_2 added cements with 5% and 10% concentrations (5% TiO_2 and 10% TiO_2) at the 6th week of testing (Fig. 4a). The last ones performed even worse than the reference samples (REF-P). This could be associated to the slightly but signif-

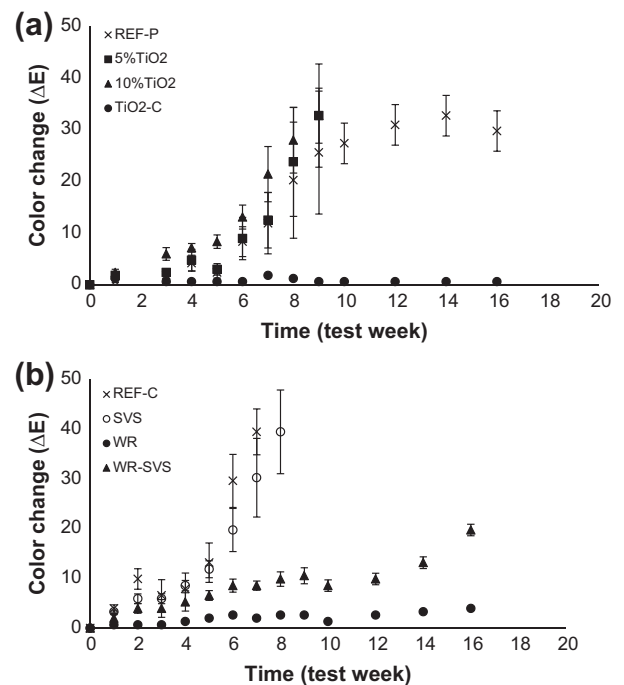


Fig. 5. Evolution of the color changes (ΔE) on different (a) TiO_2 containing cement pastes and (b) TiO_2 coated autoclaved aerated concrete samples ($n = 9$).

icant higher porosity of these samples compared to the reference ones (Table 2). Higher porosity facilitates microorganisms fixation or materials fouling [7]. Another reason could be the inactivation of the added photocatalytic nanoparticles by the hydration products of the cement. The TiO_2 used (Kemira Chemicals, Finland) in both samples (5% TiO_2 and 10% TiO_2) was the same that showed in

Table 2
Physical properties of all test specimens.

Cementitious material	Test specimen code	Porosity (%) $n = 3$	Roughness (μm) $n = 200$	TiO ₂ content (weight basis)
Cement paste (w/c = 0.5)	REF-P	32.4 ± 0.5	8.7 ± 3.1	0%
	5%TiO ₂	35.1 ± 0.1	7.7 ± 1.2	5% ^b
	10%TiO ₂	36.7 ± 0.1	7.8 ± 1.6	10% ^b
	TiO ₂ -C	40.8 ± 0.5	9.8 ± 3.2	1.4%
Autoclaved aerated concrete	REF-C	76.8 ± 1.4 ^a	39.9 ± 16.3	–
	SVS	76.8 ± 1.4 ^a	38.3 ± 16.3	0.06 ^b g cm ^{−2}
	WR-SVS	76.8 ± 1.4 ^a	30.0 ± 10.6	0.06 ^b g cm ^{−2}
	WR	76.8 ± 1.4 ^a	45.2 ± 22.7	–



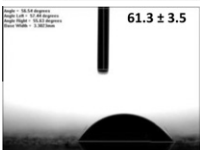

^a Porosity was determined on the substrate (autoclaved aerated concrete) without coating application and it was assumed equal for all coated samples.

^b The TiO₂ specific surface was confirmed to be 100 m² g^{−1} using a volumetric N₂-gas adsorption method (BET, Belsorp-mini, Japan). Analogously, TiO₂ was confirmed to be anatase type by performing a X-ray diffractometric analysis (Siemens D5000, Germany).

Table 3
Quantitative mineral composition of the commercially available TiO₂ containing cement used for samples (TiO₂-C).

Name	Amount (wt.%)
Calcium aluminate	2.8
Alite–Hatrurite	55.2
Belite–Larnite	15.7
Anhydrite	2.4
Gypsum	1.7
Titanium dioxide (anatase)	1.4
Others/amorphous	20.8

Table 4
Water contact angle measurements at 1 and 10 s from samples TiO₂-C and REF-P.

Sample	Water contact angle ^a (°)	
	1 s	10 s
REF-P	 90.6 ± 8.4	 70.9 ± 15.3
TiO ₂ -C	 61.3 ± 3.5	 51.8 ± 2.3

^a Water contact angle averages and standard deviations are calculated from measurements on three drops (right and left angles) on each sample. The images presented are representative and are only for one measurement.

recent work efficient toluene removal from air when applied as coatings [10,11], where these blocking phenomena are inexistent or much less pronounced.

Based on the color changes and the human perception scale of these changes (Fig. 5a), ‘not visible’ color changes ($\Delta E \leq 0.2$) were produced on samples prepared with TiO₂-C while ‘very large’ color changes ($\Delta E > 30$) were measured on the 5%TiO₂ and 10%TiO₂ samples. Although the TiO₂ content (1.4% anatase – Table 3) of the TiO₂-C samples was lower than that in the prepared TiO₂ added cement samples (5% and 10%), the better performance as

antifouling strategy is presumably associated to the following reasons:

- The existence of an important amorphous phase (20.8%) probably due to the presence of water proofing compounds. Although these compounds do not develop self-cleaning activity, they can significantly decrease wettability or water ingress. This can be observed in Table 4 by comparing the decrease in the water contact angles at 1 and 10 s on samples TiO₂-C and REF-P.
- The presence of an additive in the amorphous phase which avoids the formation of the blocking action produced by the hydration products around the TiO₂ particles. The latter act as nucleation sites for cement hydration products (Fig. 6 [30]).
- The mixing procedure (mechanical) used by the cement producer during TiO₂ loading of the samples (TiO₂-C) guarantees better dispersion of the TiO₂ particles by avoiding their flocculation.

3.3. Algal fouling on autoclaved aerated concrete samples

Regarding the coating WR-SVS applied on autoclaved aerated concrete samples, the algal coverage area shows a reduction of 20% after 16 test weeks (Figs. 3b–5b), compared to the non-coated (REF-C) and the vacuum saturation technique (SVS) coated samples. Apart from the reduction in coverage area, also a delay in time of almost 8 weeks is noticed with respect to algal fouling rate. However, ‘very large’ color changes ($\Delta E = 20$) were observed on the WR-SVS samples (Fig. 5b) after 16 weeks. Hence, the combination of TiO₂ photocatalysis and the water repellent in the same coating did not enhance the algicidal efficiency in comparison with the sole application of the water repellent (WR) which underwent lower color changes ($3.0 \leq \Delta E \leq 6.0$), and a smaller algal coverage (10%). Experiments on coating WR-SVS indicated that the evidenced algal growth was due to TiO₂ photocatalytic degradation of the water repellent layer, as can be observed from the decrease in the contact angle (from $120^\circ \leq \text{WCA} \leq 140^\circ$ to $\text{WCA} \approx 40^\circ$) after exposure to UV-A irradiation during more than 24 h (Fig. 7). The degradation of the organic groups of silane may result in the presence of hydrophilic silica on top of the TiO₂ particles. This silica layer may act as final substrate for algal growth preventing further photoactivity of the TiO₂ particles. The last result confirms that the water repellent layer (silane based) was degraded by TiO₂ photocatalysis which is responsible for the elimination of the anti-fouling properties of the WR-SVS coating at the end of the algal growth experiment. Therefore, more research should be focused on the selection of the water repellent combined strategy to enhance the algicidal effect.

4. Conclusions

In this research, evaluation of three different TiO₂ added cements and one TiO₂ coating was conducted using an accelerated algal growth test set-up with UV-A irradiation and using *Chlorella vulgaris* as the algae specie. Monitoring of these TiO₂ based strategies was conducted by visual inspections, color change measurements and quantification of the algal coverage during 16 weeks (4 months). Results proved that samples prepared with the commercially available TiO₂ containing cement (TiO₂-C) did not show visible algal growth ($\Delta E \leq 0.2$) and almost no significant coverage (0.1%) within the time frame of these experiments, making this material an excellent candidate for avoiding algal fouling on new building facades. On the contrary, cement paste samples containing 5% and 10% TiO₂ (5%TiO₂ and 10%TiO₂) did not appear to be efficient to avoid algal growth. The TiO₂ based coating (WR-SVS) evidenced a significant reduction of the coverage rate (8 weeks)

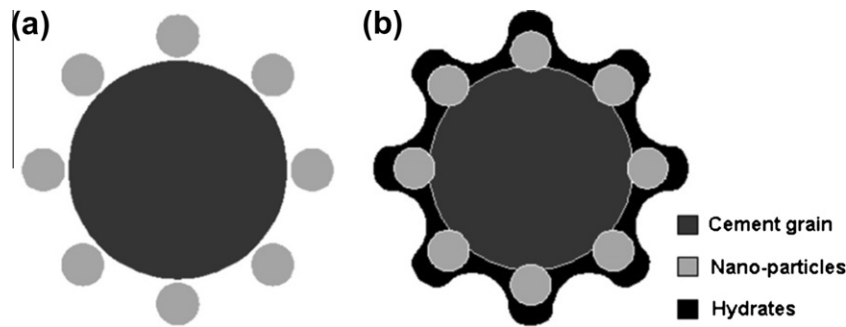


Fig. 6. State of nano-TiO₂ in cement matrix: (a) dry particle mixture and (b) after hydration [30].

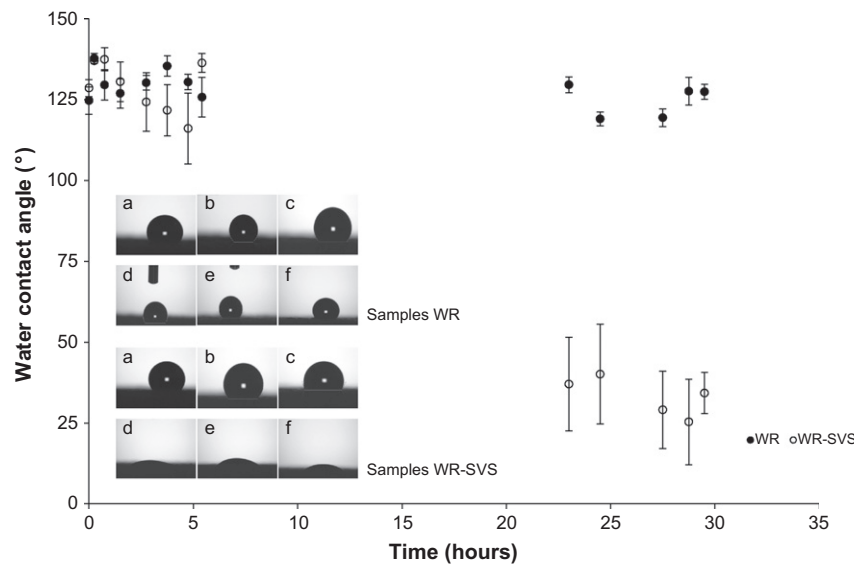


Fig. 7. Evolution of the water contact angles ($n = 6$) of test samples containing water repellent (WR and WR-SVS) before (time 0) and after UV-A irradiation. Includes images from the evolution of different water drops (5 µl) before and during UV-A irradiation 0 h (a), 0.75 h (b), 2.75 h (c), 27.5 h (d), 28.75 h (e), 29.5 h (f) on samples WR and WR-SVS.

and algal coverage (20%) during this test, but it was less efficient than the coating containing only water repellent (WR). This is shown to be caused by the photocatalytic degradation of the silane containing WR layer in the WR-SVS coating. Although more research should be conducted to enhance the algicidal activity in a combined photocatalytic and water repellent strategy, the results obtained with both the commercially available TiO₂ containing cement (TiO₂-C) and the WR-(SVS) coatings are promising. These novel materials have the potential to reduce cleaning maintenance activities and thus contribute to the sustainability of concrete buildings.

Acknowledgements

The authors would like to thank the funding given by Ghent University via the BOF Grant 01W04308. We are also grateful to Ghent University personnel who supported us in many different tasks. Similarly, the special collaboration with the Flanders Materials Center – FLAMAC (Belgium) to conduct the water contact angle measurements is acknowledged. Finally, the kind supplies of the TiO₂ and TiO₂ containing cement for these experiments by Kemira Chemicals (Finland) and CBR (Belgium) are greatly acknowledged.

References

- [1] Ohama Y, Van Gemert D. Introduction. In: Ohama Y, Van Gemert D, editors. Application of titanium dioxide photocatalysis to construction materials. State-of-the-art report of the RILEM technical committee 194-TDP. Springer; 2011. p. 1–4 [Chapter 1].
- [2] De Belie N. Microorganisms versus stony materials: a love-hate relationship. Mater Struct 2010;43:1191–202.
- [3] Giannantonio DJ, Kurth JC, Kurtis KE, Sobecky PA. Molecular characterizations of microbial communities fouling painted and unpainted concrete structures. Int Biodeterior Biodegrad 2009;63:30–40.
- [4] Gaylarde ChC, Gaylarde PM. A comparative study of the major microbial biomass of biofilms on exteriors of buildings in Europe and Latin America. Int Biodeterior Biodegrad 2005;55:131–9.
- [5] Tiano P. Biodeterioration of cultural heritage: decay mechanisms and control methods. In: Proceedings of ARIADNE 9: workshop on historic materials and their diagnostics; 2009. p.1–37 <http://www.arcchip.cz/w09/w09_tiano.pdf>.
- [6] Russel AD, Chopra I. Understanding antibacterial action and resistance. 2nd ed. Chichester (UK): Ellis Horwood; 1996.
- [7] De Muynck W, Maury Ramirez A, De Belie N, Verstraete W. Evaluation of strategies to prevent algal fouling on white architectural and cellular concrete. Int Biodeterior Biodegrad 2009;63:679–89.
- [8] Charola AE, Delgado Rodrigues J, Vale Anjos M. An unsatisfactory case of water repellents applied to control biomineralization. In: De Clercq H, Charola AE, editors. Proceedings hydrophobe V: water repellent treatment of building materials, Germany; 2008. p. 117–27.
- [9] Kus H. Long-term performance of water repellants on rendered autoclaved aerated concrete. PhD. thesis. Stockholm (Sweden), Royal Institute of Technology; 2002.
- [10] Maury Ramirez A, Demeestere K, De Belie N. Photocatalytic activity of titanium dioxide nanoparticle coatings applied on autoclaved aerated concrete: effect of

- weathering on coating physical characteristics and gaseous toluene removal. *J Hazard Mater* 2012;218–25.
- [11] Maury Ramirez A, Demeestere K, De Belie N, Mäntylä T, Levänen E. Titanium dioxide coated cementitious materials for air purifying purposes: preparation, characterization and toluene removal potential. *Build Environ* 2010;45:832–8.
- [12] Demeestere K, Dewulf J, De Witte B, Beeldens A, Van Langenhove H. Heterogeneous photocatalytic removal of toluene from air on building materials enriched with TiO₂. *Build Environ* 2008;43:406–14.
- [13] Hüsken G, Hunger M, Brouwers HJH. Experimental study of photocatalytic concrete products for air purification. *Build Environ* 2009;44:2463–74.
- [14] Chen J, Poon Ch. Photocatalytic activity of titanium dioxide modified concrete materials – influence of utilizing recycled glass cullets as aggregates. *Environ Manage* 2009;90:3436–42.
- [15] Poon CS, Cheung E. NO removal efficiency of photocatalytic paving blocks prepared with recycled materials. *Constr Build Mater* 2007;21:1746–53.
- [16] Giannantonio DJ, Kurth JC, Kurtis KE, Sobecky PA. Effects of concrete properties and nutrients on fungal colonization and fouling. *Int Biodeterior Biodegrad* 2009;63:252–9.
- [17] Fonseca AJ, Pina F, Macedo MF, Leal N, Romanowska-Deskins A, Laiz L, et al. Anatase as an alternative application for preventing biodeterioration of mortars: evaluation and comparison with other biocides. *Int Biodeterior Biodegrad* 2010;64:388–96.
- [18] Maury Ramirez A, De Belie N. Evaluation of the algacide activity of titanium dioxide on autoclaved aerated concrete. *J Adv Oxid, Technol* 2009;12:100–4.
- [19] Linkous CA, Carter GJ, Locuson DB, Ouellette AJ, Slattery DK, Smith LA. Photocatalytic inhibition of algae growth using TiO₂, WO₃, and cocatalyst modifications. *Environ Sci Technol* 2000;34:4754–8.
- [20] Maury A, De Belie N. State of the art of TiO₂ containing cementitious materials: self-cleaning properties. *Mater Constr* 2010;60:33–50.
- [21] Gladis F, Schumann R. Influence of material properties and photocatalysis on phototrophic growth in multi-year roof weathering. *Int Biodeterior Biodegrad* 2011;65:36–44.
- [22] Hashimoto K, Fujishima A, Murasawa S. Water purification using efficient TiO₂ photocatalyst: application to aquarium water filter systems. In: Rose TL, Rudd E, Murphy O, Conway BE, editors. *Proceedings of the symposium on water purification by photocatalytic, photoelectrochemical, and electrochemical processes*. USA: The Electrochemical Society; 1994. p. 368–71.
- [23] Peller JR, Whitman RL, Griffith S, Harris P, Peller C, Scalzitti J. TiO₂ as a photocatalyst for control of the aquatic invasive alga, *Cladophora*, under natural and artificial light. *Photochem Photobiol A: Chem* 2007;186:212–7.
- [24] Hong J, Ma H, Otaki M. Controlling algal growth in photo-dependent decolorant sludge by photocatalysis. *J Biosci Bioeng* 2005;99:592–7.
- [25] American Society for Testing and Materials ASTM. ASTM F 710-08 Standard practice for preparing concrete floors to receive resilient flooring; 2008.
- [26] American Society for Testing and Materials ASTM. ASTM C 1202-02 Standard test method for electrical indication of concrete's ability to resist chloride ion penetration; 2002.
- [27] British Standards Organization BS. BS 1134 British standard method for the assessment of surface texture (Parts 1 and 2); 2010.
- [28] Rasband W. Image J Software; 2011 <<http://rsb.info.nih.gov/ij/>>.
- [29] Zhang Y. Methodology for aesthetic repair and rehabilitation of architectural concrete. Master thesis, Johannesburg (South Africa), University of Johannesburg, 2005.
- [30] Chen J, Kou SC, Poon CS. Photocatalytic cement-based materials: comparison of nitrogen oxides and toluene removal potentials and evaluation of self-cleaning performance. *Build Environ* 2011;46:1827–33.